



## ORIGINAL RESEARCH ARTICLE

# (Curcumin+sildenafil) enhances the efficacy of 5FU and anti-PD1 therapies in vivo

Paul Dent<sup>1</sup> | Laurence Booth<sup>1</sup> | Jane L. Roberts<sup>1</sup> | Andrew Poklepovic<sup>2</sup> | John F. Hancock<sup>3</sup>

<sup>1</sup>Departments of Biochemistry and Molecular Biology, Virginia Commonwealth University, Richmond, Virginia

<sup>2</sup>Departments of Biochemistry and Medicine, Virginia Commonwealth University, Richmond, Virginia

<sup>3</sup>Department of Integrative Biology and Pharmacology, University of Texas Health Science Center, Houston, Texas

## Correspondence

Paul Dent, Department of Biochemistry and Molecular Biology, Virginia Commonwealth University, Richmond, VA 23298-0035.  
Email: paul.dent@vcuhealth.org

## Funding information

Commonwealth Health Research Board, Grant/Award Number: 236-04-18; Massey Cancer Center; Universal Inc. Chair in Signal Transduction Research

## Abstract

We have extended our analyses of (curcumin+sildenafil) biology. The drug combination caused vascularization and degradation of mutant K-RAS that correlated with reduced phosphorylation of ERK1/2, AKT T308, mTORC1, mTORC2, ULK1 S757, STAT3, STAT5, and NF $\kappa$ B and increased phosphorylation of eIF2 $\alpha$ , ATM, AMPK $\alpha$ , ULK1 S317; all concomitant with elevated ATG13 S318 phosphorylation and autophagosome formation. Prior studies with drug combinations utilizing sildenafil have delineated an ATM-AMPK-ULK1 S317 pathway and an AKT-mTOR-ULK1 S757 pathway as modules which control ATG S318 phosphorylation and autophagosome formation. The knockdown of PKG reduced cell killing as well as reducing drug-enhanced phosphorylation of ATM, AMPK $\alpha$ , and ATG13. In the absence of PKG, no significant increase in ULK1 S317 phosphorylation was observed. In a Beclin1-dependent fashion, the drug combination reduced the expression of multiple histone deacetylase (HDAC) proteins, including HDAC2 and HDAC3. Molecular knockdown of HDAC2, HDAC3, and especially (HDAC2+HDAC3) significantly reduced the expression of PD-L1 and elevated expression of Class I human major histocompatibility complex. In vivo, (curcumin+sildenafil) enhanced the efficacy of 5-fluorouracil against CT26 colorectal tumors. Prior exposure of established CT26 tumors to (curcumin+sildenafil) significantly enhanced the efficacy of a subsequently administered anti-PD-1 antibody. Collectively our data argue that (curcumin+sildenafil) has the potential in several settings to be an efficacious neoadjuvant therapy for colon cancer.

## KEYWORDS

5FU, autophagy, chaperone, colon cancer, HDAC, immunotherapy

**Abbreviations:** AIF, apoptosis inducing factor; AMPK, AMP-dependent protein kinase; ca, constitutively active; CMV, empty vector plasmid or virus; CUR, curcumin; dn, dominant negative; ER, endoplasmic reticulum; ERK, extracellular regulated kinase; HDAC, histone deacetylase; IP, immunoprecipitation; MHCA, human major histocompatibility complex class I A; mTOR, mammalian target of rapamycin; ODC, ornithine decarboxylase; PD-L1, programmed death ligand 1; PDE, phospho-diesterase; PI3K, phosphatidylinositol 3 kinase; SCR, scrambled; STAT, signal transducers and activators of transcription; VEH, vehicle.

## 1 | INTRODUCTION

We recently demonstrated at physiologic concentrations of the dietary compound curcumin synergized with the PDE5 inhibitor sildenafil (Viagra<sup>®</sup>) to kill a diverse variety of GI tumor cells (Roberts, Andrew Poklepovic, & Booth, 2017). Curcumin as a single agent has low solubility in water and a very poor PK/PD in patients (Dei Cas & Ghidoni, 2019; Lao, Ruffin, & Normolle, 2006; Vareed et al., 2008). Chen et al. (2001)

reported that an 8 g single dose of curcumin had a  $C_{max}$  of approximately 1.7  $\mu$ M. Based on this data, we chose to use 2  $\mu$ M curcumin for our in vitro studies. More recently, the bioavailability and in vivo stability of curcumin have been significantly improved by incorporating the compound into lecithin micelles, with safe  $C_{max}$  concentrations in the low micromolar range and with a much longer plasma half-life (Asher et al., 2017; Cuomo et al., 2011). For our upcoming Phase II clinical studies in colon cancer with curcumin and sildenafil, we are collaborating with Idena, who make a clinically tested GMP lecithin curcumin formulation called "Meriva<sup>®</sup>" (Asher et al., 2017; Cuomo et al., 2011). Administration of 400 mg Meriva<sup>®</sup> results in plasma  $C_{max}$  concentrations of approximately 200–500 nM. Hence, we plan to dose at 3 g curcumin/day for our clinical studies.

In our prior work, we determined that curcumin and sildenafil interacted to kill GI tumor cells and that this was mediated via the extrinsic and intrinsic apoptosis pathways and additionally, that killing required autophagosome formation. In vivo, curcumin and sildenafil interacted to suppress the growth of colon cancer tumors in a syngeneic mouse host. Multiplex analyses of plasma taken after drug exposure indicated that the level of PDGF was significantly increased following (curcumin+sildenafil) exposure which was associated with elevated PDGFR $\beta$  phosphorylation. Cells isolated from in vivo treated (curcumin+sildenafil) tumors were resistant to in vitro (curcumin+sildenafil) exposure; a resistance that was abrogated by the PDGFR $\beta$  inhibitor and FDA-approved colon cancer therapeutic regorafenib (Roberts et al., 2017).

Findings from our laboratory, using a variety of drug combinations, all of which strongly induce autophagosome formation, has demonstrated that autophagy can facilitate the degradation of a wide variety of signal transduction proteins (Booth, Roberts, Rais, et al., 2017; Booth, Roberts, Poklepovic, et al., 2017; Booth, Roberts, Sander, et al., 2018; Booth, Roberts, Rais et al., 2018; Booth, Roberts, Rais, Poklepovic, & Dent, 2018; Booth, Roberts, Kirkwood, Poklepovic, & Dent, 2018; Booth, Roberts, Poklepovic, et al., 2018; Booth, Roberts, Rais, et al., 2019; Booth, Roberts, Poklepovic, & Dent, 2019). Thus, we have shown autophagy can contribute to the degradation of receptor tyrosine kinases and mutant RAS proteins and histone deacetylase proteins (HDAC). One aspect of HDAC downregulation data was that reduced expression of HDACs resulted in altered expression of proteins involved with tumor cell immunogenicity, and the sensitivity of tumor cells to checkpoint inhibitory immunotherapeutic antibodies. And, in several model systems, including melanoma and NSCLC, our in vitro hypotheses were confirmed in vivo.

Colorectal cancer (CRC), is considered by the medical oncology field to be a "cold" tumor type that rarely responds to checkpoint immunotherapy antibodies (Kalyan, Kircher, Shah, Mulcahy, & Benson, 2018; Spallanzani et al., 2018), with the exception of microsatellite unstable CRC tumors where the response rates are profound (Kalyan et al., 2018). Our prior work with curcumin and sildenafil had demonstrated that the agents interacted to suppress the growth of CT26 mouse colorectal tumors in their syngeneic C57/BL6 mouse host. The plasma of drug-treated mice contained greater

levels of M-CSF, G-CSF, PDGF, CXCL9, IL-12, and reduced levels of KC (mouse equivalent to IL-8), CXCL-1, and CCL5. Reduced CXCL1 levels correlate with decreased colorectal tumor growth and suppressed tumorigenic growth of K-RAS mutant colon cancer cells (le Rolle et al., 2015). Furthermore, high CXCL1 expression is known to be a poor prognostic biomarker in metastatic colon cancer (Oladipo et al., 2011). The present studies were performed to provide additional mechanistic understanding as to how curcumin and sildenafil interact to kill and to determine whether the (curcumin+sildenafil) combination could enhance the efficacy of an anti-PD1 antibody.

## 2 | MATERIALS AND METHODS

### 2.1 | Materials

Sildenafil and 5FU were purchased from Selleck Chem (Houston, TX). Curcumin was purchased from Sigma-Aldrich (St. Louis, MO). Trypsin-EDTA, Dulbecco's modified Eagle's medium (DMEM), RPMI, penicillin-streptomycin were purchased from GIBCOBRL (GIBCOBRL Life Technologies, Grand Island, NY). Tumor cell lines were purchased from the ATCC and were not further validated beyond that claimed by ATCC. Cells were repurchased every approximately 6 months. Plasmids were purchased from Addgene, (Cambridge, MA). Commercially available validated short hairpin RNA molecules to knockdown RNA/protein levels were from Qiagen (Valencia, CA; e.g., knock down data shown pictorially and numerically in Figures 1–3). The prevalidated smart-pool siRNA molecules used were siSCR (SI03650318), ATM (SI00604737), cathepsin B (1027416), BAX (GS581), BAK (GS578); AMPK $\alpha$  (GS5562), BIM (GS10018), BAD (GS572), Beclin1 (GS8678), ATG5 (GS9474), CD95 (GS355), AIF (GS9131), eIF2 $\alpha$  (GS83939), FADD (GS8772), ULK-1 (GS8408), ATG13 (GS9776). The antibodies used in these studies were AIF (5318), BAX (5023), BAK (12105), BAD (9239), BIM (2933), BAK1 (12105), Beclin1 (3495), cathepsin B (31718), CD95 (8023), FADD (2782), eIF2 $\alpha$  (5324), P-eIF2 $\alpha$  S51 (3398), ULK-1 (8054), P-ULK-1 S757 (14202), P-AMPK $\alpha$  S51 (2535), AMPK $\alpha$  (2532), P-ATM S1981 (13050), ATM (2873), ATG5 (12994), mTOR (2983), P-mTOR S2448 (5536), P-mTOR S2481 (2974), ATG13 (13468), MCL-1 (94296), BCL-XL (2764), P-AKT T308 (13038), P-ERK1/2 (5726), P-STAT3 Y705 (9145), P-p65 NF $\kappa$ B S536 (3033), p62 (23214), LAMP2 (49067) all from Cell Signaling Technology; P-ULK-1 S317 (3803a) from Abgent; P-ATG13 S318 (19127) from Novus Biologicals. Antibodies directed against RAS proteins: Thermo-Fisher (Waltham, MA) N-RAS PA5-14833; K-RAS PA5-44339. Control IgG and anti-PD-1 endotoxin-free antibodies were purchased from Bio-Xcell (West Lebanon, NH; Booth, Roberts, Rais, et al., 2017; Booth, Roberts, Poklepovic, et al., 2017; Booth, Roberts, Sander, et al., 2018; Booth, Roberts, Rais, Cutler, et al., 2018, Booth, Roberts, Rais, Poklepovic, et al., 2018; Booth, Roberts, Kirkwood, et al., 2018; Booth, Roberts, Poklepovic, et al., 2018; Booth, Roberts, Rais et al., 2019; Booth, Roberts, Poklepovic, et al., 2019).

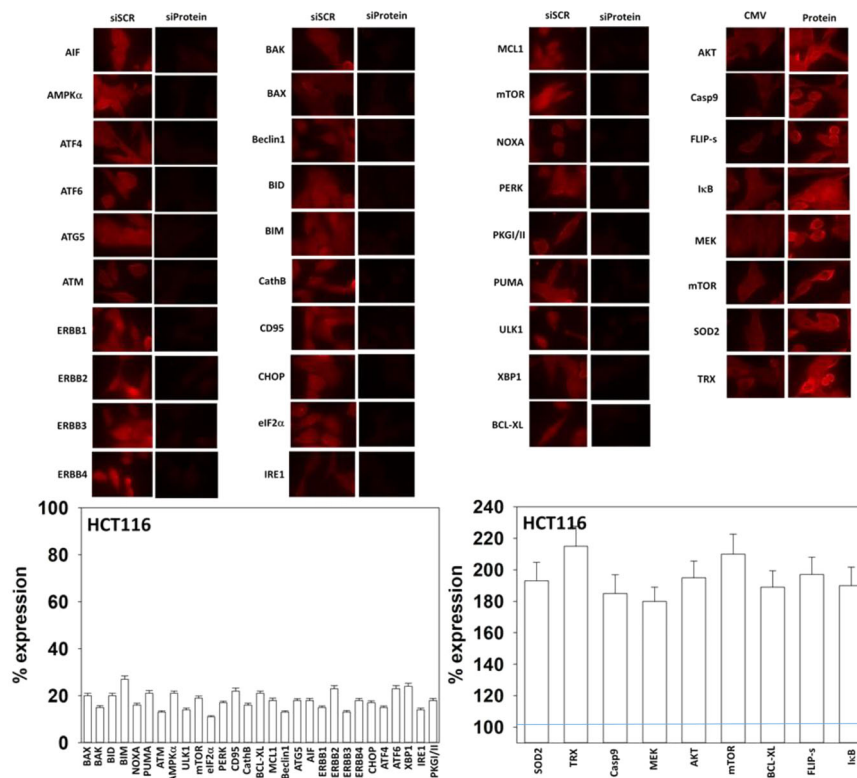


**FIGURE 1** Representative images of proteins whose expression was knocked down or overexpressed in the manuscript, using HCT116 colorectal cancer cells as an example. Cells, 24 hr after plating, were transfected with a scrambled control small interfering RNA (siRNA) or with validated siRNA molecules to knock down the indicated proteins. Alternatively, cells were transfected with an empty vector plasmid (CMV) or with a plasmid to over-express the indicated protein. Twenty-four hours after transfection, cells were fixed in place and immunostaining performed using validated antibodies, corrected for ERK2 total loading. The percentage change in expression comparing scrambled control/CMV versus knock down siRNA or plasmid overexpression treated is indicated numerically under each image. ( $n = 3$  independent assessments from 40 cells per image  $\pm$  standard deviation). The images below were taken at 60 $\times$  magnification. ERK, extracellular regulated kinase

## 2.2 | Methods

### 2.2.1 | Culture and in vitro exposure of cells to drugs

All cell lines were cultured at 37 $^{\circ}$ C (5% v/v CO<sub>2</sub>) in vitro using DMEM supplemented with 5% (v/v) fetal calf serum. For short term cell killing assays, immunofluorescence studies, cells were plated at a density of  $3 \times 10^3$  per cm<sup>2</sup> ( $\sim 2 \times 10^5$  cells per well of a 12-well plate). In vitro drug treatments were generally from a 100 mM stock solution of each drug and the maximal concentration of vehicle carrier (VEH; dimethyl sulfoxide) in media was 0.02% (v/v). All drug stock solutions were stored at  $-80^{\circ}$ C. Cells were not cultured in reduced serum media during any study in this manuscript.

### 2.2.2 | Transfection of cells with siRNA or with plasmids

#### For plasmids

Cells were transfected 24 hr after plating. Plasmids expressing a specific mRNA (or siRNA) or appropriate vector control plasmid DNA

was diluted in 50  $\mu$ l serum-free and antibiotic-free medium (one portion for each sample). Concurrently, 2  $\mu$ l Lipofectamine 2000 (Invitrogen), was diluted into 50  $\mu$ l of serum-free and antibiotic-free medium (one portion for each sample). Diluted DNA was added to the diluted Lipofectamine 2000 for each sample and incubated at room temperature for 30 min. This mixture was added to each well/dish of cells containing 200  $\mu$ l serum-free and antibiotic-free medium for a total volume of 300  $\mu$ l, and the cells were incubated for 4 hr at 37 $^{\circ}$ C. An equal volume of 2 $\times$  medium was then added to each well. Cells were incubated for 24 hr, then treated with drugs.

#### Transfection for siRNA

Cells from a fresh culture growing in the log phase as described above were transfected 24 hr after plating. Before transfection, the medium was aspirated, and serum-free medium was added to each plate. For transfection, 10 nM of the annealed siRNA, the positive sense control doubled stranded siRNA targeting glyceraldehyde 3-phosphate dehydrogenase or the negative control (a "scrambled" sequence with no significant homology to any known gene sequences from mouse, rat or human cell lines) were used. Ten nanomolar siRNA (scrambled or experimental) was diluted in serum-free media. Four microliters Hiperfect (Qiagen) was added to this mixture and

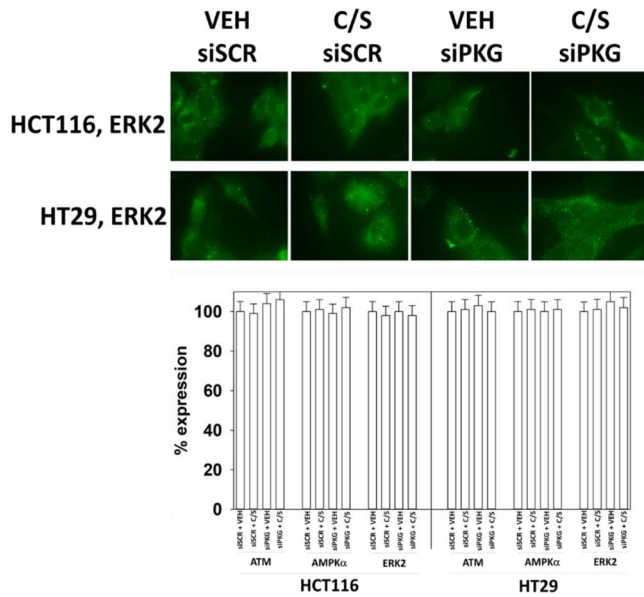


**FIGURE 2** Control knock down images; knock down of PKG nor treatment with (curcumin+sildenafil) alters the basal expression of ATM, AMPK $\alpha$ , or ERK2. Cells, 24 hr after plating, were transfected with a scrambled control siRNA or with validated siRNA molecules to knock down PKGI and PKGII. Twenty-four hours after transfection, cells were treated for 6 hr with vehicle control or with (curcumin [2  $\mu$ M]+sildenafil [2  $\mu$ M]). Cells were fixed in place and immunostaining performed using vendor validated antibodies to assess the expression of ATM, AMPK $\alpha$ , and ERK2. The percentage change in expression comparing scrambled control versus knock down siRNA treated is indicated numerically under each image. ( $n = 3$  independent assessments from 40 cells per image  $\pm$  standard deviation). The images below were taken at 60 $\times$  magnification. ATM, ataxia telangiectasia mutated; AMPK $\alpha$ , AMP-dependent protein kinase; ERK, extracellular regulated kinase

the solution was mixed by pipetting up and down several times. This solution was incubated at room temp for 10 min, then added drop-wise to each dish. The medium in each dish was swirled gently to mix, then incubated at 37 $^{\circ}$ C for 2 hr. Serum-containing medium was added to each plate, and cells were incubated at 37 $^{\circ}$ C for 24 hr before then treated with drugs (0–24 hr). Additional immunofluorescence/live–dead analyses were performed at the indicated time points. Figures 1–3 show immuno-fluorescent imaging of a range of cell proteins following specific siRNA knockdown/or the use of a “scrambled” sequence with no significant homology to any known gene sequences from mouse, rat or human cell lines.

### 2.2.3 | Animal studies

Studies were performed according to USDA regulations under the VCU IACUC protocol AD20008. Immunocompetent BALB/c mice (~20 g) were injected with  $1 \times 10^6$  CT26 cells into their rear flank (eight animals per treatment group  $\pm$  standard deviation [SD]). Tumors were permitted to form for 7 days with tumors at that time exhibiting a mean volume of approximately 40 mm $^3$ . Although exposure of mice to 5FU resulted in less grooming behavior, no treatment in any of the three mouse studies resulted in a significant reduction in animal body mass.

### 2.2.4 | Immunotherapy animal study

Mice were treated by oral gavage once every day QD for 5 days with vehicle (Cremophore; 63013; Sigma-Aldrich, St Louis, MO); with sildenafil (5 mg/kg) and on Days 1–5; or with curcumin (50 mg/kg)

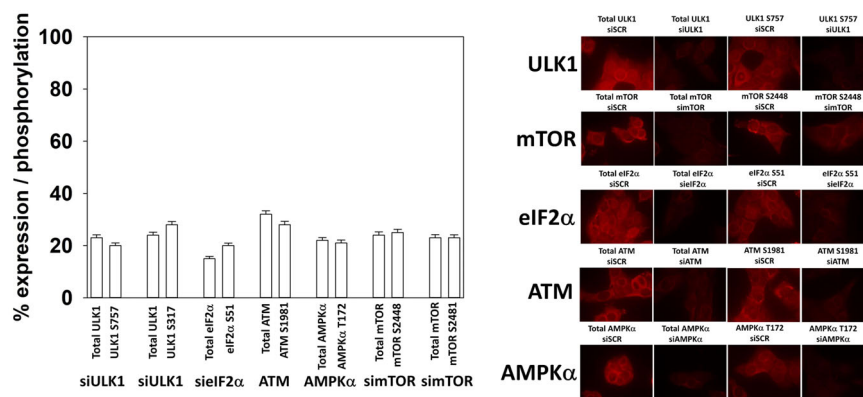


**FIGURE 3** Knock down of protein expression correlates with reduced immunoreactivity of phospho-specific antibodies; bar graphs. Cells were transfected with a scrambled control small interfering RNA (siRNA) or with validated siRNA molecules to knock down the indicated proteins. Twenty-four hour after transfection, cells were fixed in place and immunostaining performed using vendor validated total expression antibodies and with phospho-specific antibodies for the same protein, corrected for ERK2 total loading. The percentage change in expression comparing scrambled control versus knock down siRNA treated is indicated numerically under each image. ( $n = 3$  independent assessments from 40 cells per image  $\pm$  standard deviation). The images were taken at 60 $\times$  magnification. ATM, ataxia telangiectasia mutated; AMPK $\alpha$ , AMP-dependent protein kinase ERK, extracellular regulated kinase; mTOR, mammalian target of rapamycin

combined on Days 1–5. On Days 4 and 6, animals were administered IP either a control IgG or with an anti-PD1 (both 50 mg/kg). After cessation of drug treatment tumors are again calipers as indicated in the figure and tumor volume was assessed up to 25 days later.

### 2.2.5 | 5FU/curcumin + sildenafil animal study

Animals were grouped and treated for 28 days with vehicle control (Q 5 days per week); (curcumin [50 mg/kg]+sildenafil [5 mg/kg]; Q 5 days per week); 5-fluorouracil (25 mg/kg; Q 1 day per week); and curcumin+sildenafil+5FU. The volume of the tumors was measured every 3–4 days during and following drug treatments. After cessation of drug treatment at Day 28, tumors are calipered, and tumor volume was assessed up to 15 days later.

### 2.2.6 | Detection of cell death by trypan blue

Trypan blue exclusion was used to assess cell viability at each experimental time point. Floating cells were isolated along with attached cells that were harvested by trypsinization with Trypsin/EDTA for approximately 3 min at 37°C. Following isolation, the total cell population for each experimental point was assessed for cell viability.

### 2.2.7 | Detection of protein expression and protein phosphorylation by in-cell western blot analysis using a hermes WiScan microscope

The Hermes WiScan wide-field microscope (<https://idea-bio.com/products/wiscan-hermes/>) was developed by IDEA Bio-Medical, a commercial off-shoot of the Weitzman Institute in Rehovot, Israel. The machine combines high-quality optics with a high-quality computer-driven microscope stage, and with dedicated software, for example, to analyze the immunofluorescent staining intensity of individual cells, that is true in-cell western blot analysis (Figures 1–3). Although the machine can be used as a traditional microscope with glass slides, the majority of data sets obtained in our laboratory have used 96-well plates. Cells ( $4 \times 10^3$ ) were plated into 96-well plates and allowed to grow overnight.

A typical experiment proceeds thus, three independent thaws/cultures of a particular tumor cell type are subcultured into individual 96-well plates. Twenty-four hours after plating, the cells are transfected with a control plasmid or a control siRNA, or with plasmids to express various proteins or validated siRNA molecules to knock down the expression of various proteins. After another 24 hr, the cells are ready for drug exposure(s). At various time-points after the initiation of drug exposure, cells are fixed in place with permeabilization. Standard immunofluorescent blocking procedures are employed, followed by incubation of different wells with a variety of validated primary antibodies. The next morning, after washing,

fluorescent-tagged secondary antibodies are added to each well; in general, we have found that using more than two tagged antibodies in each well results in poorer data/image quality. After 3 hr of incubation, the secondary antibody is removed, the cells washed again, and are hydrated with phosphate buffered saline before microscopic examination. Based on the experiment, cells are visualized at either 10× magnification for bulk assessments of immunofluorescent staining intensity or at 60× magnification for assessments of protein or protein–protein colocalization.

For studies at 10× magnification, the operator selects which fluorescent antibody will be assessed first, that is in the red or green channel, and then focuses the microscope in a vehicle control transfection control well. The operator then outlines for the computer controlling the microscope “what is a cell.” In other words, the operator manually inputs the criteria for each specific tumor cell line segregating away detection of what is obvious debris or a staining artifact. The operator then sets how many cells per well are to be assessed for their immunofluorescent staining intensity; we initially selected 40 cells per well but have now moved to assess 100. The computer/microscope then determines the background fluorescence in the well and in parallel randomly determines the mean fluorescent intensity of those 100 cells; the operator is provided with this mean intensity value. Of note for scientific rigor is that the operator does not personally manipulate the microscope to examine specific cells; the entire fluorescent accrual method is independent of the operator. Once the entire plate has been scanned for one of the secondary antibodies, the second secondary antibody with a different fluorescence range can similarly be used to define the mean intensity value in each well. Once data from the first set of plated cells has been obtained, the second and third sets of plated cells can be processed through the machine. Thus, we obtain three independent sets of fluorescence data from the three individual cultures, with 300 cells under each condition being assessed ( $\pm$ standard deviation [SD]).

### 2.2.8 | Data analysis

Comparison of the effects of various treatments was performed using one-way analysis of variance and a two-tailed Student's *t*-test using Sigma-Plot and Sigma-Stat software. Statistical examination of in vivo utilized log rank statistical analyses between the different treatment groups. Differences with a  $p < .05$  were considered statistically significant. Experiments shown are the means of multiple individual points from multiple experiments ( $\pm$ standard error of mean).

## 3 | RESULTS

HCT116 human colorectal cancer cells naturally express a mutated K-RAS allele and we transfected these cells with plasmids to express the fusion proteins K-RAS V12–GFP and K-RAS V12–RFP so as to more clearly visualize K-RAS localization after (curcumin+sildenafil)



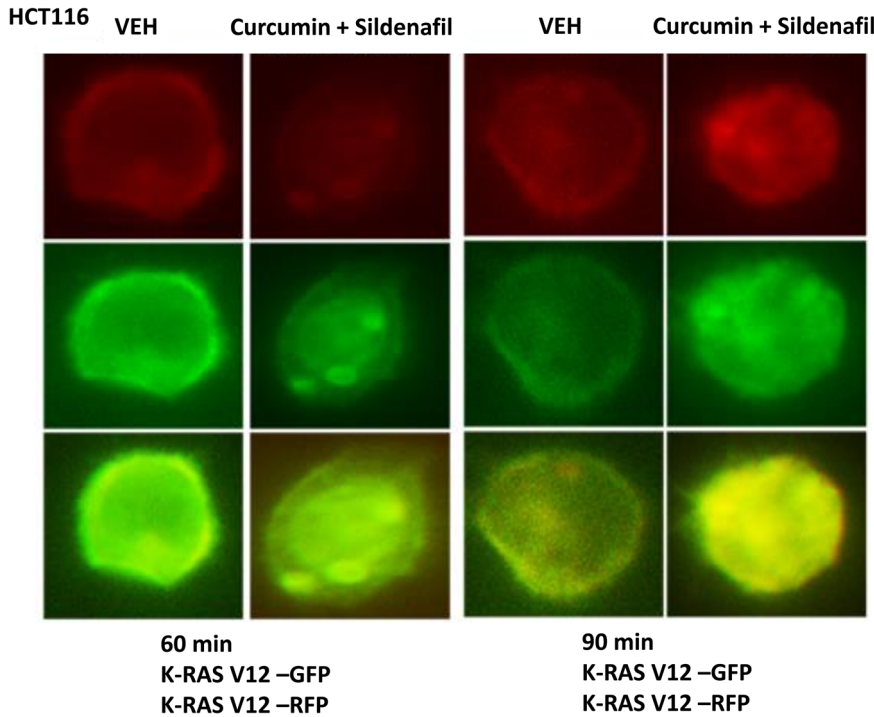


**FIGURE 4** Exposure to (curcumin +sildenafil) reduces the expression of mutant K-RAS. HCT116 human colorectal cancer cells were transfected with plasmids to express K-RAS V12-GFP and K-RAS V12-RFP, and 24 hr after transfection cells were treated with vehicle control or with (curcumin [2 μM]+sildenafil [2 μM]). Cells were imaged at 60× magnification 60 and 90 min after curcumin/sildenafil exposure. Representative images from multiple studies are presented (n = 3). VEH, vehicle

exposure. Both GFP and RFP tagged proteins were expressed to control for any potential off-target effects of differing tag expression or loss of GFP signal due to quenching in acidic endosomes. Treatment of the transfected HCT116 cells with (curcumin+sildenafil) caused the GFP fluorescence of the K-RAS V12-GFP protein to become punctate, in agreement with our immunostaining data (Figure 4). The GFP and RFP tagged K-RAS proteins colocalized at these early timepoints.

We next examined alterations in cell signaling caused by [curcumin + sildenafil]. Six hours after exposure, the expression of

PDGFRβ and ERBB1 were increased in both HCT116 colon cells that express a mutant K-RAS and HT29 colon cancer cells that express a mutant B-RAF (Figure 5a,b). Representative 10× magnification images of the cells, with numerical fluorescence intensity quantitation, are presented (Figure 6). In HT29 cells, the levels of ERBB2 and ERBB3 were also increased whereas in HCT116 cells only ERBB3 expression was modestly enhanced. Receptor tyrosine phosphorylation is a biomarker for elevated receptor activity. In HCT116 cells (curcumin+sildenafil) the levels of PDGFRβ phosphorylation mirrored those for total PDGFRβ expression whereas in HT29 cells the

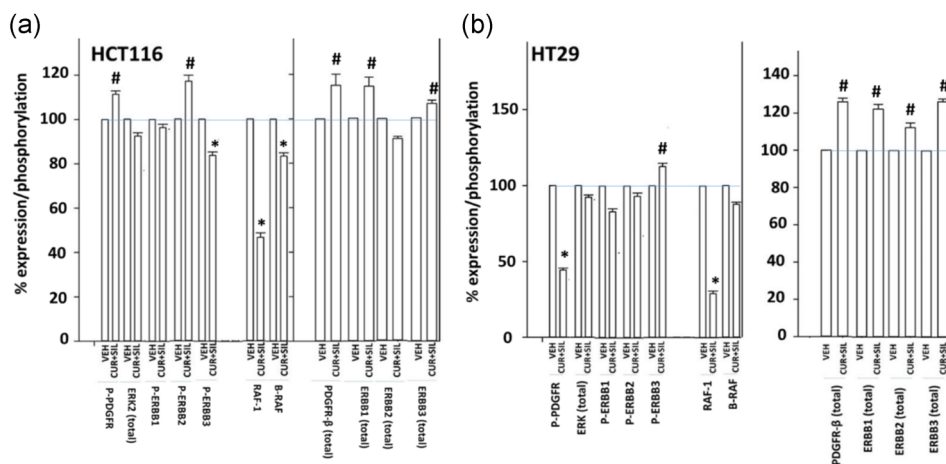


**FIGURE 5** Exposure of GI tumor cells to (curcumin+sildenafil) causes compensatory enhanced signaling through ERBB family receptors and the PDGFRβ. (a,b) GI tumor cells were treated for 6 hr with vehicle control or with (curcumin [2 μM]+sildenafil [2 μM]). Cells were fixed in place and immunostaining performed to determine the expression and phosphorylation of ERBB1, ERBB2, ERBB3, PDGFRβ, and the expression of RAF-1 and B-RAF. The percentage change in phosphorylation comparing vehicle control versus drug exposed is presented. (n = 3 independent treatments from 40 random cells per treatment ± standard deviation). #p < .05 greater than vehicle control value; \*p < .05 less than vehicle control value

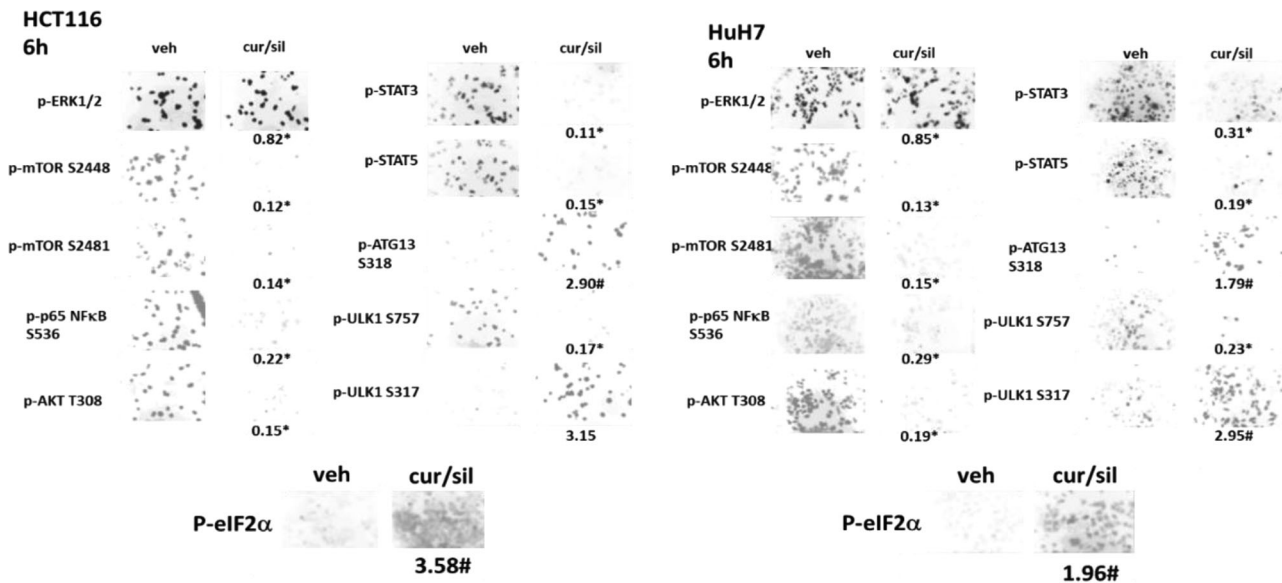


**FIGURE 6** Pictorial and numeric presentation of curcumin plus sildenafil effects. GI tumor cells were treated for 6 hr with vehicle control or with (curcumin [2  $\mu$ M]+sildenafil [2  $\mu$ M]). Cells were fixed in place and immunostaining performed to determine the expression and phosphorylation of the indicated proteins. Representative images of the stained cells at 10 $\times$  magnification are presented. The percentage change in phosphorylation comparing vehicle control versus drug exposed is presented under each image. ( $n = 3$  independent treatments from 40 random cells per treatment  $\pm$  standard deviation) # $p < .05$  greater than corresponding vehicle control value; \* $p < .05$  less than vehicle control value

phosphorylation of PDGFR $\beta$  was significantly reduced, despite increased receptor expression. In HCT116 cells the phosphorylation of ERBB2 was elevated whereas ERBB2 expression trend towards reduced levels. The phosphorylation and expression of ERBB3 was increased in HT29 cells. In both cell types, the drug combination reduced the expression of RAF-1 but not of B-RAF. Thus, it is possible that upon downregulating RAS function/expression, that RAF-1 associated with RAS is also being degraded.

Exposure of GI tumor cells transfected with scrambled control to (curcumin + sildenafil) modestly reduced the activity of ERK1/2 but strongly reduced the phosphorylation/activity of mTORC1, mTORC2, AKT, STAT3, STAT5, and p65 NF $\kappa$ B (Figure 7a,b). One possibility why the decline in ERK1/2 phosphorylation was not greater may be due to the fact that although (curcumin + sildenafil) reduces mutant K-RAS expression, it also activated upstream receptor tyrosine kinases that could act to partially maintain ERK1/2 phosphorylation. These events were associated with activation of ataxia telangiectasia mutated (ATM) kinase and the AMP-dependent protein kinase (AMPK), the dephosphorylation of the mTOR substrate ULK1 S757, which facilitates ULK1 activation; enhanced phosphorylation of the AMPK substrate ULK1 S317, which further promotes ULK1 activation, and with both events correlating with a approximately two-fold increase in phosphorylation of the ULK1 substrate and gatekeeper to autophagosome formation ATG13 S318.

In GI tumor cells transfected to knock down PKG1 and PKGII, ERK1/2 phosphorylation either remained stable or slightly declined. The ability of (curcumin+sildenafil) to reduce the phosphorylation of mTORC1, mTORC2, AKT, STAT3, STAT5, and p65 NF $\kappa$ B and to enhance the phosphorylation of eIF2 $\alpha$  and ULK1 S757 was

significantly less in the absence of PKGI/II, equating to a approximately 60% inhibition of the effect (Figure 7a,b; right panel graphical data). Most notable, however, was that in the absence of PKGI/II the elevation in both ATM and AMPK $\alpha$  phosphorylation was reduced by 75–80% and the phosphorylation of ULK1 S317 was reduced by greater than 90% that is ULK S317 phosphorylation was abolished (Figure 7a,b; right panel graphical data). In control studies, the basal expression levels of ERK2, AMPK $\alpha$ 1/2, and ATM were not altered by PKGI/II knock down (Figure 2). Knock down of PKGI/II significantly reduced the lethality of (curcumin+sildenafil; Figure 8a). Knock down of eIF2 $\alpha$  or to a lesser extent ATM prevented the drug combination from inactivating mTOR and from elevating ATG13 S318 phosphorylation (Figure 8b,c). This data argues that sildenafil-induced PKG activation plays a primary role in activating the ATM-AMPK-ULK1 S317 signaling pathway which is essential for efficient tumor cell killing.

Knock down of the autophagy-regulatory proteins ATG5 or Beclin1 suppressed drug combination lethality (Figure 9a). Knock down of ATM, AMPK $\alpha$ , ULK1, CD95, FADD, PERK, eIF2 $\alpha$ , AIF, and cathepsin B; all significantly suppressed (curcumin+sildenafil) lethality (Figure 9b). In both HCT116 and HT29 cells, overexpression of BCL-XL or GRP78 reduced killing as did expression of dominant negative caspase 9 or activated mTOR (Figure 9c). Collectively, our data demonstrates that (curcumin+sildenafil) causes activation of multiple protective RTKs, but also causes inactivation of AKT and mTOR and activation of the AMPK and ULK1 which results in autophagosome formation. Autophagosome formation causes the expression of multiple chaperone proteins to be reduced which is essential for mTOR inactivation and eIF2 $\alpha$  phosphorylation.

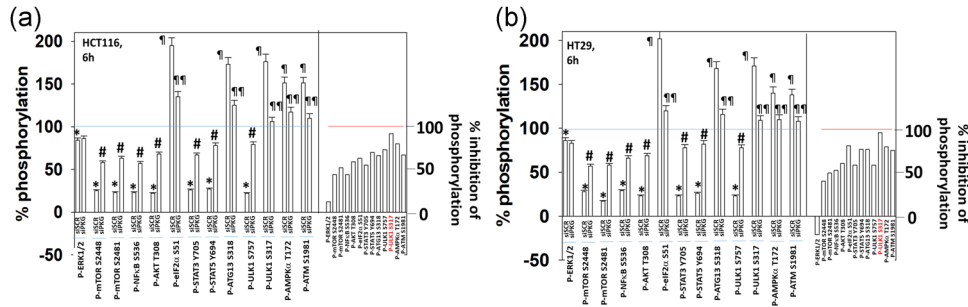


**FIGURE 7** (Curcumin+sildenafil) interact via PKG and eIF2 $\alpha$  to regulate signaling. (a, b) Colon cancer cells were transfected with a scrambled siRNA control or with siRNA molecules to knock down the expression of PKGI and PKGII. Twenty-four hours after transfection, cells were treated with vehicle control or (curcumin [2  $\mu$ M]+sildenafil [2  $\mu$ M]) in combination for 6 hr. Cells were fixed in place and immunostaining performed to determine the phosphorylation of the indicated proteins. ( $n = 3$  independent treatments from 40 random cells per treatment  $\pm$  standard deviation) #  $p < .05$  greater than vehicle control value; \*  $p < .05$  less than vehicle control value. Right bar graph: the percentage reduction or enhancement of phosphorylation caused by knock down of PKGI/II was calculated. siRNA, small interfering RNA

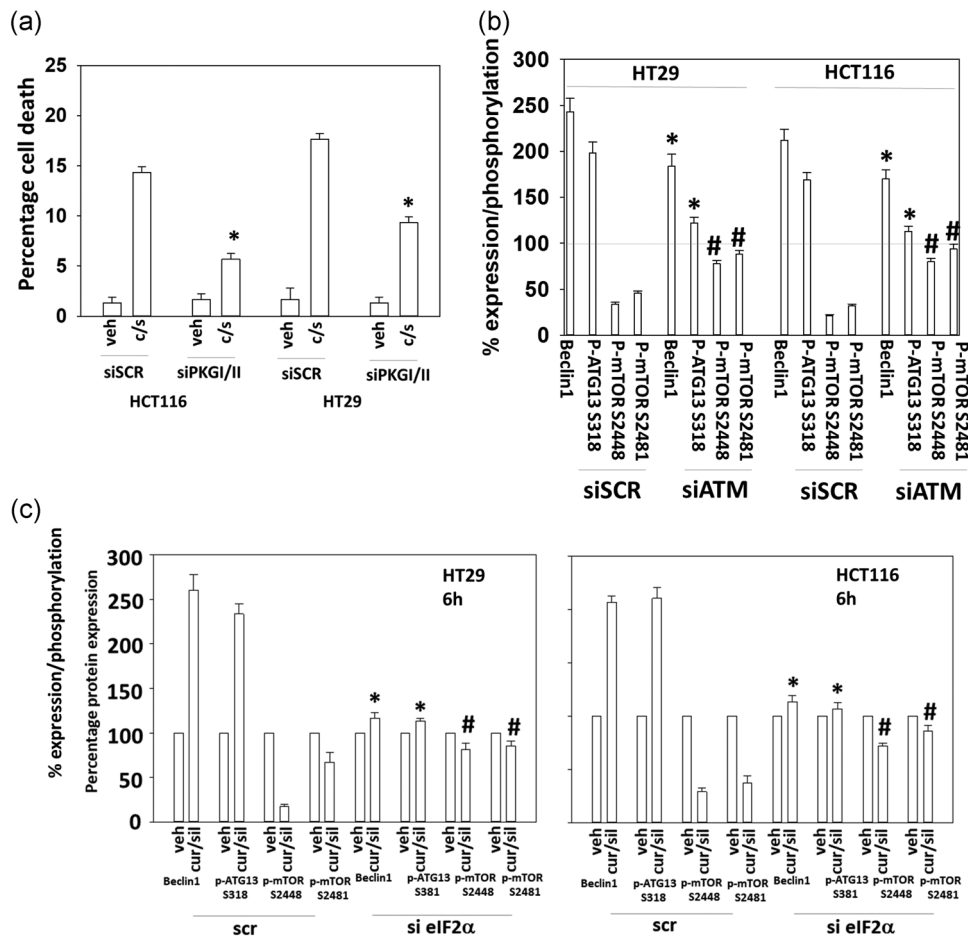


**FIGURE 8** Signaling by PKG and ATM, and reduced eIF2 $\alpha$  function play important regulatory roles following curcumin plus sildenafil exposure. (a) Cells were transfected with a scramble siRNA control or with siRNA molecules to knock down PKGI and PKGII. Twenty-four hour after transfection, cells were treated with vehicle control or with (curcumin [2  $\mu$ M]+sildenafil [2  $\mu$ M]) for 24 hr. Cell viability was determined by trypan blue exclusion assays ( $n = 3 \pm SD$ ) \*  $p < .05$  less than corresponding value in siSCR transfected cells. (b,c) Cells were transfected with a scramble siRNA control or with siRNA molecules to knock down eIF2 $\alpha$  or to knock down ATM. Twenty-four hours after transfection, cells were treated with vehicle control or with (curcumin [2  $\mu$ M]+sildenafil [2  $\mu$ M]) for 6 hr. Cells were fixed in place and immunostaining performed to determine the phosphorylation of the indicated proteins. The percentage change in phosphorylation comparing vehicle control versus drug exposed is indicated under each image. ( $n = 3$  independent treatments from 40 random cells per treatment  $\pm$  standard deviation). #  $p < .05$  greater than vehicle control value; \*  $p < .05$  less than vehicle control value. ATM, ataxia telangiectasia mutated; SD, standard deviation; siRNA, small interfering RNA





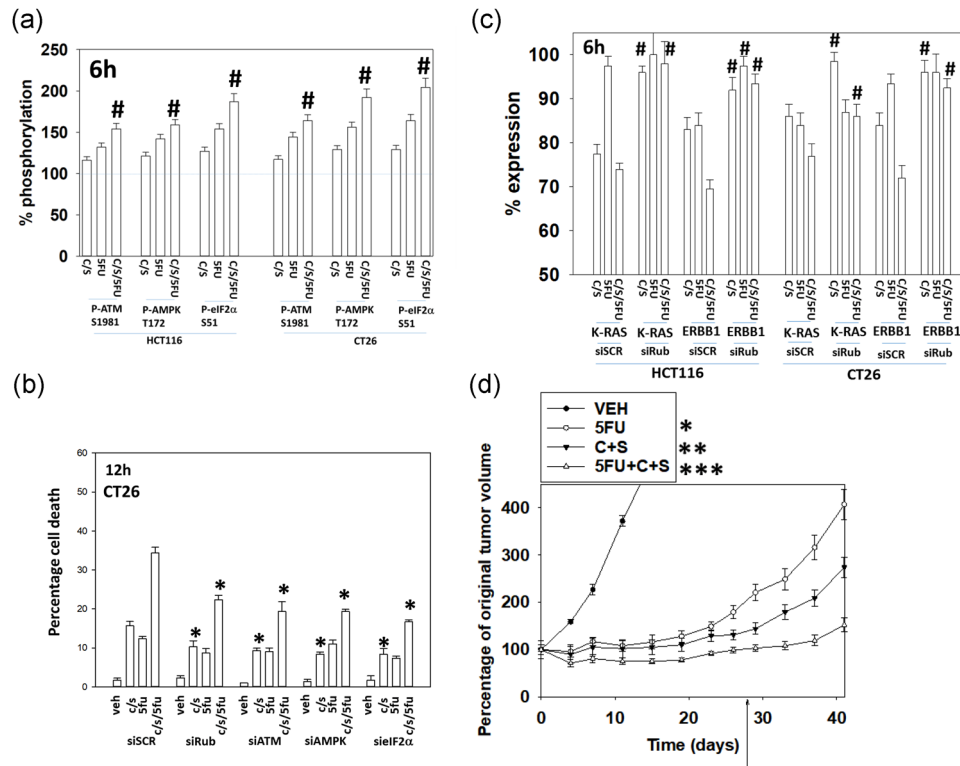


**FIGURE 10** (Curcumin + sildenafil) interact with 5-fluorouracil to kill colon cancer cells via ER stress, LC3-associated phagocytosis (LAP), and DNA damage signaling. (a) Colon cancer cells were treated with vehicle control, (curcumin [2  $\mu$ M]+sildenafil [2  $\mu$ M]), 5FU (50  $\mu$ M) or the drugs in combination for 6 hr. Cells were fixed in place and immunostaining performed to determine the phosphorylation of the indicated proteins. The percentage change in phosphorylation comparing vehicle control versus drug exposed as indicated under each image. ( $n = 3$  independent assessments from 40 cells per image  $\pm$  standard deviation [SD]) # $p < .05$  greater than 5FU value. (b) CT26 and HCT116 cells were transfected with a scrambled control siRNA or with siRNA molecules to knock down the expression of Rubicon, ATM, AMPK or eIF2 $\alpha$ . Twenty-four hours after transfection, cells were treated with vehicle control, (curcumin [2  $\mu$ M]+sildenafil [2  $\mu$ M]), 5FU (50  $\mu$ M) or the drugs in combination for 24 hr. Cell viability was determined by trypan blue exclusion assays ( $n = 3 \pm$  SD) \* $p < .05$  less than the corresponding value in siSCR transfected cells. (c) Colon cancer cells were transfected with scrambled control siRNAs or with siRNAs to knock down the expression of Rubicon. Twenty-four h after transfection, cells were treated with vehicle control, (curcumin [2  $\mu$ M]+sildenafil [2  $\mu$ M]), 5FU (50  $\mu$ M) or the drugs in combination for 6 hr. Cells were fixed in place and immunostaining performed to determine the expression of K-RAS and ERBB1. The percentage change in expression comparing vehicle control versus drug exposed as indicated under each image. ( $n = 3$  independent assessments from 40 cells per image  $\pm$  SD) # $p < .05$  greater than the corresponding value in siSCR cells. (d) CT26 tumors were grown in the flanks of BALB/c mice until tumors reached a volume of approximately 40 mm<sup>3</sup>. Animals were grouped and treated for 28 days with vehicle control (Q 5 days per week); (curcumin [25 mg/kg]+sildenafil [5 mg/kg]; Q 5 days per week); 5-fluorouracil (25 mg/kg; Q 1 day per week); curcumin+sildenafil+5FU. The volume of the tumors was measured every 3–4 days during and following drug treatments ( $n = 8$  per group  $\pm$  SD) \* $p < .05$  less than vehicle control; \*\* $p < .05$  less than 5FU alone. AMPK, AMP-dependent protein kinase

protein Beclin1 prevented (curcumin+sildenafil) from reducing HDAC expression (Figure 11b). In our recent prior publications, we have linked reduced HDAC expression via autophagy, using siRNA techniques, to altered expression of proteins that can regulate tumor cell immunogenicity to checkpoint inhibitory antibodies. Exposure of GI tumor cells to (curcumin+sildenafil) rapidly reduced the protein expression of programmed death ligand 1 (PD-L1), programmed death ligand 2 (PD-L2) and ornithine decarboxylase (ODC). In parallel, it increased the protein levels of human major histocompatibility complex class I A (MHCA; Figure 11c). Knock down of HDAC2 and HDAC3 recapitulated the changes in PD-L1 and MHCA expression as was observed using (curcumin + sildenafil; Figure 12a). Based on these findings, we performed an animal study using CT26 colorectal cancer cells growing in their syngeneic C57/BL6 mouse host. CT26

tumors were formed in mice and animals exposed to (curcumin +sildenafil) followed by exposure to an anti-PD-1 antibody. Exposure of tumors to (curcumin+sildenafil) significantly reduced tumor growth; an effect that was significantly further enhanced by the administration of the anti-PD-1 antibody (Figure 12b).

## 4 | DISCUSSION

The present studies were performed to further define the molecular mechanisms by which curcumin interacts with the PDE5 inhibitor sildenafil to kill GI tumor cells. The mechanisms by which the combination interacted to cause cell death were multi-factorial. Signaling by the extrinsic and intrinsic apoptosis pathways accounted

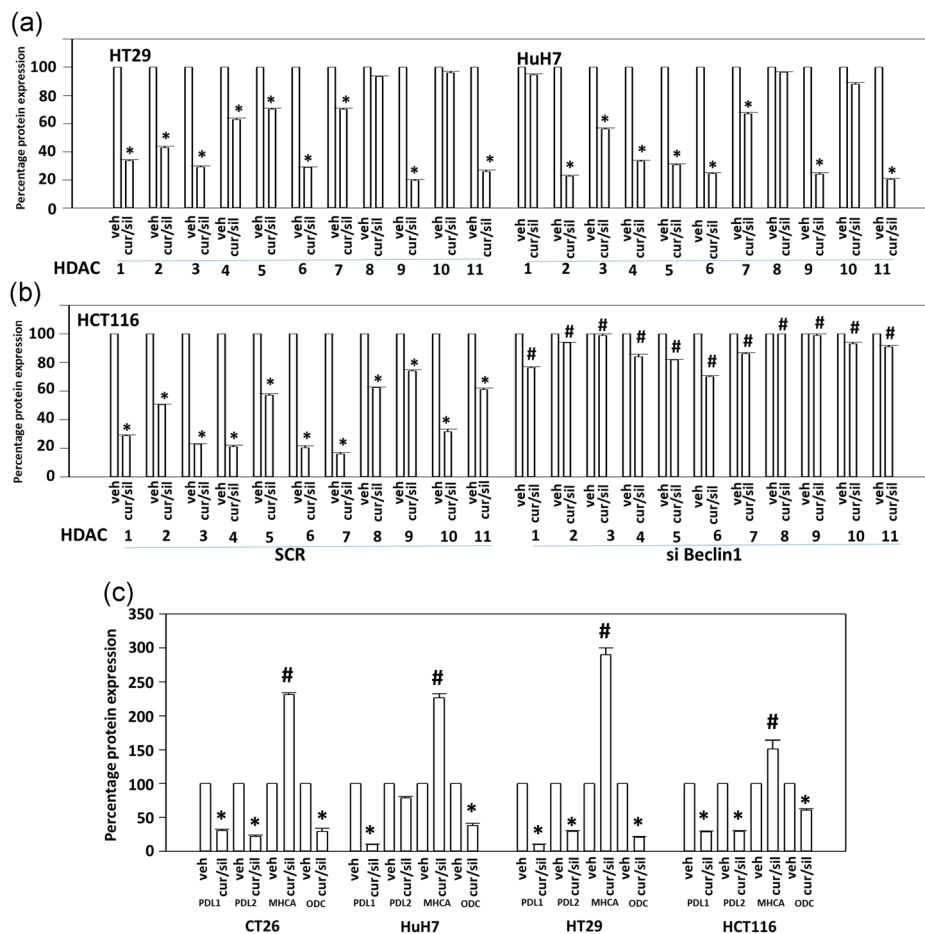


**FIGURE 11** Exposure to (curcumin+sildenafil) reduces the expression of PD-L1, PD-L2, and ODC, and enhances MHCA levels. (a) HT29 (colon) and HuH7 (liver) cancer cells were treated with vehicle control or with [curcumin (2  $\mu$ M)+sildenafil (2  $\mu$ M)] for 6 hr. Cells were fixed in place and immunostaining performed to determine the expression of the indicated HDAC proteins. The fold change in expression comparing vehicle control versus drug exposed is indicated numerically under each image. ( $n = 3$  independent assessments from 40 cells per image  $\pm$  standard deviation [SD]). \* $p < .05$  less than vehicle control. (b) HCT116 cells were transfected with a scrambled siRNA molecule (siSCR) or with an siRNA to knock down the expression of Beclin1 (siBeclin1). Twenty-four hour after transfection cells were treated with vehicle control or with (curcumin [2  $\mu$ M]+sildenafil [2  $\mu$ M]) for 6 hr. Cells were fixed in place and immunostaining performed to determine the expression of the indicated HDAC proteins. The fold change in HDAC protein expression comparing vehicle control versus drug exposed is indicated numerically under each image. ( $n = 3$  independent assessments from 40 cells per image  $\pm$  SD). \* $p < .05$  less than vehicle control; # $p < .05$  greater than the corresponding value in SCR cells. HDAC, histone deacetylase; ODC, ornithine decarboxylase; MHCA, human major histo-compatibility complex class I A; PD-L, programmed death ligand

for approximately 50% of the observed killing. The drugs interacted to inactivate mTORC1 and mTORC2 activity and increased Beclin1 levels and the numbers of autophagosomes and autolysosomes in cells in a PERK-eIF2 $\alpha$ -dependent fashion. Knock down of Beclin1 or ATG5 suppressed killing. Curcumin and sildenafil reduced the expression of the protective proteins MCL-1 and BCL-XL and reduced the levels of the reactive oxygen species detoxifying enzymes thioredoxin and superoxide dismutase 2, all in an eIF2 $\alpha$ -dependent fashion. Curcumin and sildenafil interacted in a greater than additive fashion to increase the levels of reactive oxygen species and knock down of thioredoxin or SOD2 enhanced killing and overexpression of thioredoxin or SOD2 suppressed killing.

Several of the GI tumor cell types used in the present study, for example, HCT116 and CT26, express a mutant GTPase inactivated K-RAS protein (Fernández-Medarde, & Santos, 2011; Thompson &

Lyons, 2005). Locked into the GTP-bound mode, oncogenic RAS constitutively activates the ERK1/2 pathway that mediates proliferation and survival, (Kurada & White, 1998; Meier & Evan, 1998). In several studies, we have shown that neratinib causes the proteolytic degradation of mutated forms of K-RAS and N-RAS. Others have observed sildenafil mediated activation of PKG leads to down-regulation of K-RAS (Cho et al., 2016). In the present study, we have shown that (curcumin+sildenafil) interacted to reduce mutant K-RAS protein levels. Further, we have shown the punctate vascularization of K-RAS V12 using GFP and RFP tagged forms of the protein (Qi et al., 2014).

The (curcumin+sildenafil)-mediated reduction in K-RAS expression, along with ERBB1 expression, was further enhanced by the CRC maintenance-phase standard of care drug 5FU. Knockdown of the LAP-regulatory protein Rubicon prevented the (curcumin+sildenafil)

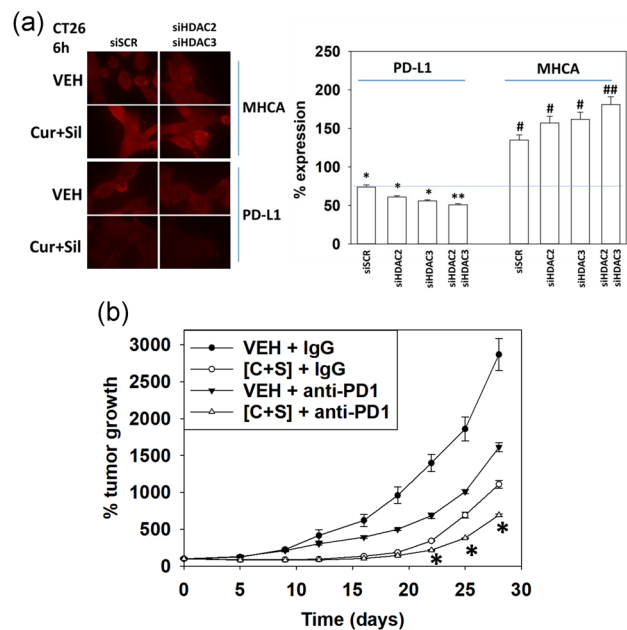


**FIGURE 12** (Curcumin+sildenafil) exposure enhances the efficacy of an anti-PD1 antibody. (a) GI tumor cells were treated for 6 hr with vehicle control or (sildenafil [2  $\mu$ M]+curcumin [2  $\mu$ M]) combined. Cells were fixed in place and immunostaining performed to determine the expression of the indicated immunoregulatory proteins. The fold change in expression comparing vehicle control versus drug exposed is indicated numerically under each image. ( $n = 3$  independent assessments from 40 cells per image  $\pm$  standard deviation [SD]). \* $p < .05$  less than vehicle control; # $p < .05$  greater than vehicle control. (b) CT26 cells were transfected with a scrambled small interfering RNA (siRNA) control or with siRNA molecules to knock down HDAC2, HDAC3 or to knock down both HDAC proteins. Twenty-four hour after transfection cells were fixed in place and staining performed to determine the expression of PD-L1 and MHCA. ( $n = 3$  independent assessments from 40 cells per image  $\pm$  SD). \* $p < .05$  less than vehicle control; # $p < .05$  greater than vehicle control. (c) CT26 mouse colon cancer cells that express a mutant K-RAS were implanted into the flanks of syngeneic male BALB/c mice. Mice were treated QD for 5 days with vehicle control or with (curcumin [25 mg/kg] + sildenafil [5 mg/kg]). On Days 4 and 6, mice were injected immunoprecipitation with a control IgG (50 mg/kg) or an anti-PD1 IgG (50 mg/kg). Tumors were callipered, and tumor volumes determined before and following drug exposure. ( $n = 8 \pm$  standard error of mean) \* $p < .05$  less than (curcumin +sildenafil+control IgG). HDAC, histone deacetylase; MHCA, human major histo-compatibility complex class I A; siRNA, small interfering RNA; VEH, vehicle

$\pm$ 5FU mediated reduction in K-RAS and ERBB1, implicating LC3-associated phagocytosis, alongside macroautophagy, in mediating cell death signals. Treatment with (curcumin+sildenafil) was also shown to affect signaling events downstream of K-RAS. Endoplasmic reticulum stress signaling is mediated through three self-regulatory pathways: via eIF2 $\alpha$ , IRE1, and ATF6 (Hertz, 2012). Signaling by eIF2 $\alpha$  reduces transcription from many cytoprotective genes resulting in the rapid reduction of protein expression for those with short half-lives, for example, MCL-1. In agreement with the reduced expression of

multiple chaperones/cytoprotective proteins, (curcumin + sildenafil) significantly enhanced eIF2 $\alpha$  S51 phosphorylation. This led to an eIF2 $\alpha$  dependent dephosphorylation of mTOR and the mTOR substrate ULK1 S757 and the phosphorylation of ULK1 S317 which ultimately led to ULK1 activation, leading to increased ATG13 S318 phosphorylation, implicating (curcumin + sildenafil)-mediated ER stress and autophagy in the elevated levels of cell death.

Previous studies by our group have indicated that the induction of autophagy can lead to reduced expression of HDAC enzymes. In this study, (curcumin + sildenafil) downregulated HDAC1-7, HDAC9, and HDAC11 levels, an effect that was significantly reduced by Beclin1 knockdown indicating another role for autophagy in the response of cells to this drug combination. Our recent studies have linked altered HDAC expression in cancer cells to an altered expression of a number of immunogenic biomarkers predicted to enhance tumor cell immunogenicity. Exposure to [curcumin + sildenafil] rapidly decreased the expression of PD-L1, PD-L2, and ODC and increased the levels of MHCA. A 5-day treatment with (curcumin + sildenafil) reduced tumor growth and combined exposure with an anti-PD-1 antibody caused a further significant reduction in the rate of tumor growth. Collectively, the findings presented in this manuscript suggest that future clinical studies beyond our proposed Phase II trial using (curcumin + sildenafil + 5FU) would include the use of the CRC therapeutic regorafenib as well as the inclusion of checkpoint inhibitory anti-PD1 antibody in CRC patients.

## ACKNOWLEDGMENTS

The authors thank Mr. K. Owusu and Ms. R. Rais for technical assistance in the performance of these studies. Support for the present study was funded from philanthropic funding from Massey Cancer Center and the Universal Inc. Chair in Signal Transduction Research. Paul Dent acknowledges funding by the Commonwealth Health Research Board (CHRB) of Virginia.

## CONFLICT OF INTERESTS

The authors declare that there are no conflict of interests.

## AUTHOR CONTRIBUTIONS

L. B. and J. L. R. performed the studies. A. P. and J. F. H. provide advice on experimental directions and approaches to P. D. J. F. H. provided reagents. P. D. wrote the manuscript with help from A. P.

## DATA AVAILABILITY STATEMENT

Data can be provided following an appropriate request.

## ORCID

Paul Dent  <http://orcid.org/0000-0001-6948-1875>

## REFERENCES

- Asher, G. N., Xie, Y., Moaddel, R., Sanghvi, M., Dossou, K. S. S., Kashuba, A. D. M., ... Hawke, R. L. (2017). Randomized pharmacokinetic crossover study comparing 2 curcumin preparations in plasma and rectal tissue of healthy human volunteers. *Journal of Clinical Pharmacology*, *57*, 185–193.
- Booth, L., Roberts, J. L., Poklepovic, A., & Dent, P. (2019). Prior exposure of pancreatic tumors to [sorafenib + vorinostat] enhances the efficacy of an anti-PD-1 antibody. *Cancer Biology & Therapy*, *20*, 109–121.
- Booth, L., Roberts, J. L., Rais, R., Poklepovic, A., & Dent, P. (2018). Valproate augments Niraparib killing of tumor cells. *Cancer Biology & Therapy*, *19*, 797–808.
- Booth, L., Roberts, J. L., Kirkwood, J., Poklepovic, A., & Dent, P. (2018). Unconventional approaches to modulating the immunogenicity of tumor cells. *Advances in Cancer Research*, *137*, 1–15.
- Booth, L., Roberts, J. L., Rais, R., Kirkwood, J., Avogadri-Connors, F., Cutler, R. E., Jr, ... Dent, P. (2017a). [Neratinib + Valproate] exposure permanently reduces ERBB1 and RAS expression in 4T1 mammary tumors and enhances M1 macrophage infiltration. *Oncotarget*, *26*(9), 6062–6074.
- Booth, L., Roberts, J. L., Poklepovic, A., Avogadri-Connors, F., Cutler, R. E., Lalani, A. S., & Dent, P. (2017). HDAC inhibitors enhance neratinib activity and when combined enhance the actions of an anti-PD-1 immunomodulatory antibody *in vivo*. *Oncotarget*, *8*, 90262–90277.
- Booth, L., Roberts, J. L., Sander, C., Lalani, A. S., Kirkwood, J. M., Hancock, J. F., ... Dent, P. (2018). Neratinib and entinostat combine to rapidly reduce the expression of K-RAS, N-RAS, G $\alpha_q$  and G $\alpha_{11}$  and kill uveal melanoma cells. *Cancer Biology & Therapy*, *20*, 1–11. <https://doi.org/10.1080/15384047.2018.1551747>
- Booth, L., Roberts, J. L., Jr, Diala, I., Lalani, A. S., ... Dent, P. (2018). Palbociclib augments Neratinib killing of tumor cells that is further enhanced by HDAC inhibition. *Cancer Biology & Therapy*, *20*, 1–12. <https://doi.org/10.1080/15384047.2018.1507665>
- Booth, L., Roberts, J. L., Poklepovic, A., Kirkwood, J., Sander, C., Avogadri-Connors, F., ... Dent, P. (2018). The levels of mutant K-RAS and mutant N-RAS are rapidly reduced in a Beclin1/ATG5 -dependent fashion by the irreversible ERBB1/2/4 inhibitor neratinib. *Cancer Biology & Therapy*, *19*, 132–137.
- Booth, L., Roberts, J. L., Rais, R., Cutler, R. E., Jr, Diala, I., Lalani, A. S., ... Dent, P. (2019). Neratinib augments the lethality of [regorafenib + sildenafil]. *Journal of Cellular Physiology*, *234*, 4874–4887.
- Chen, A. L., Hsu, C. H., Lin, J. K., Hsu, M. M., Ho, Y. F., She, T. S., ... Wu, M. S. (2001). Phase I clinical trial of curcumin, a chemopreventive agent, in patients with high-risk or pre-malignant lesions. *Anticancer Research*, *21*: e2900.
- Cho, K. J., Casteel, D. E., Prakash, P., Tan, L., van der Hoeven, D., Salim, A. A., ... Hancock, J. F. (2016). AMPK and endothelial nitric oxide synthase signaling regulates K-ras plasma membrane interactions via cyclic GMP-dependent protein kinase 2. *Molecular and Cellular Biology*, *36*, 3086–3099.
- Cuomo, J., Appendino, G., Dern, A. S., Schneider, E., McKinnon, T. P., Brown, M. J., ... Dixon, B. M. (2011). Comparative absorption of a standardized curcuminoid mixture and its lecithin formulation. *Journal of Natural Products*, *74*, 664–669.
- Dei Cas, M., & Ghidoni, R. (2019). Dietary curcumin: Correlation between bioavailability and health potential. *Nutrients*, *11*, 2147. <https://doi.org/10.3390/nu11092147>
- Fernández-Medarde, A., & Santos, E. (2011). Ras in cancer and developmental diseases. *Genes Cancer*, *2*, 344–358.
- Hertz, C. (2012). The unfolded protein response: Controlling cell fate decisions under ER stress and beyond. *Nature Reviews, Molecular Cell Biology*, *13*, 89–102.
- Kalyan, A., Kircher, S., Shah, H., Mulcahy, M., & Benson, A. (2018). Updates on immunotherapy for colorectal cancer. *Journal of Gastrointestinal Oncology*, *9*, 160–169.
- Kurada, P., & White, K. (1998). Ras promotes cell survival in *Drosophila* by downregulating hid expression. *Cell*, *95*, 319–329.
- Lao, C. D., Ruffin, M. T., Normolle, D., Heath, D. D., Murray, S. I., Bailey, J. M., ... Brenner, D. E. (2006). Dose escalation of a curcuminoid formulation. *BMC Complementary and Alternative Medicine*, *6*, 10.
- Meier, P., & Evan, G. (1998). Dying like flies. *Dying like flies*. *Cell*, *95*, 295–298.
- Oladipo, O., Conlon, S., O'Grady, A., Purcell, C., Wilson, C., Maxwell, P. J., ... Waugh, D. J. (2011). The expression and prognostic impact of CXCL chemokines in stage II and III colorectal cancer epithelial and stromal tissue. *British Journal of Cancer*, *104*, 480–487.
- Qi, X., Xie, C., Hou, S., Li, G., Yin, N., Dong, Lepp, L. A., ... Chen, G. (2014). Identification of a ternary protein-complex as a therapeutic target for K-Ras-dependent colon cancer. *Oncotarget*, *5*, 4269–4282.
- Roberts, J. L., Andrew Poklepovic, A., & Booth, L. (2017). Curcumin interacts with sildenafil to kill GI tumor cells via endoplasmic reticulum stress and reactive oxygen/nitrogen species. *Oncotarget*, *8*, 99451–99469.
- le Rolle, A. F., Chiu, T. K., Fara, M., Shia, J., Zeng, Z., Weiser, M. R., ... Chiu, V. K. (2015). The prognostic significance of CXCL1 hypersecretion by human colorectal cancer epithelia and myofibroblasts. *Journal of Translational Medicine*, *13*, 199.
- Spallanzani, A., Gelsomino, F., Caputo, F., Santini, C., Andrikou, K., Orsi, G., ... Cascinu, S. (2018). Immunotherapy in the treatment of colorectal cancer: A new kid on the block. *J Cancer Metastasis treat*, *4*, 28.
- Thompson, N., & Lyons, J. (2005). Recent progress in targeting the Raf/MEK/ERK pathway with inhibitors in cancer drug discovery. *Current Opinion in Pharmacology*, *5*, 350–356.
- Vareed, S. K., Kakarala, M., Ruffin, M. T., Crowell, J. A., Normolle, D. P., Djuric, Z., & Brenner, D. E. (2008). Pharmacokinetics of curcumin conjugate metabolites in healthy human subjects. *Cancer Epidemiology, Biomarkers and Prevention*, *17*, 1411–1417.

**How to cite this article:** Dent P, Booth L, Roberts JL, Poklepovic A, Hancock JF. (Curcumin+sildenafil) enhances the efficacy of 5FU and anti-PD1 therapies *in vivo*. *J Cell Physiol*. 2020;1–13. <https://doi.org/10.1002/jcp.29580>